ADVANCES IN ELECTRON BEAM MELTING OF ALUMINUM ALLOYS

T. Mahale*, D. Cormier*, O. Harrysson*, and K. Ervin**

*Edward P. Fitts Department of Industrial and Systems Engineering, North Carolina State University, Raleigh NC 27695

** Department of Materials Science and Engineering, North Carolina State University, Raleigh NC 27695

Abstract

The high thermal conductivity and melt pool optical reflectivity associated with aluminum alloys can pose significant challenges for direct-metal SFF processes. The use of SFF processes to produce aluminum parts is often not cost effective relative to CNC machining for simple geometries. However, the use of SFF techniques for aluminum alloys is justified for some applications such as aerospace forgings or high surface area heat exchangers. This paper describes recent progress in processing aluminum alloys using the Electron Beam Melting process. Structure and properties will be discussed, as well challenges associated with high vapor pressure alloying elements such as zinc and magnesium.

Introduction

Interest in aluminum alloys for a wide variety of applications have increased significantly over the past two decades. Several aluminum alloys have been developed which have excellent strength to weight ratios. The relatively low melting points also make processing of these alloys more energy efficient. Aluminum alloys posses other desirable qualities such as high thermal and electrical conductivity, ductility, machinability and toughness.

Research related to layered manufacturing of aluminum has largely been supported by the aerospace industry. The components used in this industry can be classified as low volume and high reliability. Annual demands for forged aluminum components in aging aircraft is commonly in the single digits. Forging dies for these components is often difficult to locate or is missing entirely. This has spurred considerable interest among the aerospace industry for SFF techniques capable of producing aerospace grade aluminum alloy components with forged or cast properties.

Many of the commercial laser melt based systems suggest sintering of polymer coated metal powder to form a green part followed by a polymer binder burnout operation to form a denser part. After this the part can be further sintered to form a dense part. An alternative to this is infiltration of the sintered skeleton formed by after the polymer binder burnout and metal powder sintering. Sercombe et al. [1, 2] suggest improvements to the process chain for sintering and infiltration based manufacturing techniques. A resin bonded Al-6061 part was first formed using a selective laser sintering

setup. The infiltration was carried out by covering the part with alumina and magnesium powder and heating it to 540°C in the presence of nitrogen. The magnesium prevents the formation of an oxide inside the porous part and the nitrogen reacts with the aluminum to form AlN. The temperature of the furnace is raised to 570 C. The rigidity of the AlN skin permits it to be infiltrated by an aluminum alloy with a narrow melting range (Al-Si binary system is preferred due to its low viscosity when molten). At 570 C, the infiltrant melts and is absorbed into the porous part. The parts produced by this process can be considered to be comparable to investment cast parts of the same material. Souvignier et al. [3] in collaboration with Sercombe have experimented with developing a fused deposition modeling like process to make aluminum metal matrix composites. A PMMA based slurry loaded with aluminum alloy in combination with silicon carbide, carbon fiber and alumina powder is extruded through a syringe to form the base. A process similar to that described above was used to generate a dense part.

Many researchers have also experimented with electron beam based melting for the production of dense aluminum parts. Matz [4], Taminger et al. [5] and Watson et al. [6] fed a raw material wire into the melt pool generated by the electron beam. Matz's work does not make any specific reference to his group having worked on the development of the system for processing aluminum alloys. Taminger and Watson have described a low energy (15 kV) electron beam system aimed at in-orbit fabrication system. The deposition speed for this system varied between 400 mm/min to 800 mm/min while maintaining a constant wire feed rate. As expected, higher translation rate led to faster cooling and finer grain structure. Another experiment was carried out were the beam traverse speed was kept constant and the wire feed was varied between 3000 mm/min and 1500 mm/min. Higher wire feed rates led to faster cooling as the energy was distributed into melting a larger amount of material, thus producing small equiaxed grain structure. The strength of parts built on this system seem to be comparable to 2219-O alloy but the surface finish of the part is dictated by the high weld pool width and height.

Electron Beam Melting of Al 2024

2024 is an aluminum alloy whose primary alloying element is copper. It is known for its excellent fatigue performance, though it is not easily welded. 2024 Al was chosen as the first candidate for trials with the Electron Beam Melting (EBM) process due to the fact that the copper will not vaporize under vacuum substantially more or less than the aluminum. It was also readily available and relatively inexpensive.

Feasibility tests for the processing of aluminum were carried out by placing a layer of aluminum powder inside a cavity approx. 0.75 mm deep in a steel plate. The experiments were cold started by directly scanning the cavity region at 10,000 mm/s between a current ramp from 0.5-3.5 mA that was covered through 100 repeats. The first experiment itself showed evidence of sintering with light balling occurring at the surface of the powder.

Details of the initial feasibility tests are listed in Table 1. These tests were conducted to provide a starting point for the parameters prior to conducting experiments for producing a freeform part (particularly the powder preheating parameters).

Table 1 Initial Feasibility Tests for 2024 Aluminum

PlateTemp. in ˚C	Melt cycle	Pre/Postheat	Observations
Cold Start	100 reps 10,000mm/s 0.5-3.5mA 0.5mm offset	None	Sintering and minor Balling
Cold Start	100 reps 10,000mm/s 0.5-7mA 0.5mm offset	None	Cracking of sintered part followed by balling
Cold start	100 reps 10,000mm/s 0.5-4.0mA 0.5mm offset	pod 100 reps 10,000mm/s 4.0-0.5mA 0.5mm offset	Objective: slowly decrease the heat as it would permit the material to flow after it has been melted to prevent balling. This did not help and balling was still observed
Cold start	100mm/s 3.2mA 0.3mm offset	phd 100 reps 10,000mm/s 0.5-5mA	Objective: Uniformly melt the balled powder. Powder segregated into two layers. Top layer balled and bottom layer sintered
300˚C	100mm/s 3.2mA 0.3mm Offset	phd 100 reps 10,000mm/s 0.5-5mA 0.5mm offset	Objective: study the effect of a hot start. Observed that hot start did not have any significant effect on the quality of the melt
300˚C	100mm/s 1.8mA 0.3mm offset	Phd1 100 reps 10,000mm/s 0.5-5mA phd2 100 reps 10,000mm/s 2-5mA	Objective: higher sintering of powder bed to provide a more stable wettable surface to prevent baling. It was observed that the balling occurred due to sputtering during the melt process.

The next set of experiments were meant to develop parameters for freeform fabrication of aluminum parts. A standard 100 mm square, steel start plate and a slice thickness of 0.07 mm was used for manufacturing aluminum 2024 samples.

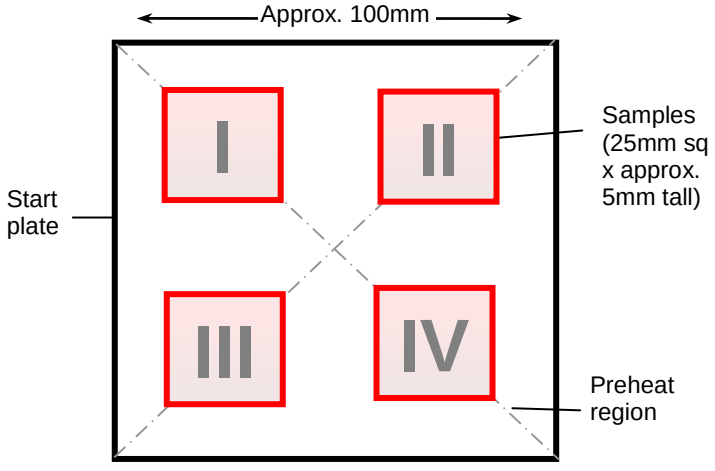

Figure 1 Configuration for small sample tests of Al 2024

As shown in Figure 1, four samples with different melt parameters were produced. The objective was to establish parameters that would produce parts that looked visually most acceptable. The details of each experiment along with qualitative observations are listed in Table 2.

The next set of experiments was to make comparisons between the ultimate tensile strength of 2024 aluminum parts produced via the EBM system and values expected from parts produced by conventional manufacturing. Tensile test specimens as dictated by ASTM-E8 standards with suitable machining allowance were fabricated via the EBM system. Rectangular coupons were fabricated and then machined to final coupon dimensions. An important observation with respect these samples can be made as follows. The coupons frequently cracked during removal from the steel build plate. The parts were removed from the start plate by tapping with a hammer and relying on the mismatched coefficient of thermal expansion between the aluminum and the steel substrate to separate the parts. This region obviously undergoes significant shear forces during cooling (mismatched CTE's) and part removal (tapping with a hammer).

Table 3 shows the different processing conditions used to make four sets of coupons, and Figure 2 shows photographs of the resulting rectangular blanks prior to machining as well as close-up photos of the top and side surfaces.

An approximate calculation of the average densities of the parts was made. The results are shown in Table 4. It is apparent that within the range of parameters used to produce these parts, the beam power had a greater influence on density than the beam velocity. It is equally clear that considerable experimentation is still needed to get the density near 100%, although it bears repeating that this was a preliminary feasibility study intended to determine the relative ease with which the EBM process could produce geometric shapes to near net shape.

Table 2 Freeform Fabrication Experimental Procedure for 2024 Aluminum

Plate Temp	Preheat	Sample I	Sample II	Sample III	Sample IV
480˚C	50 reps 10,000 mm/s 0.5-6mA	1.8mA, 100mm/s	2.5mA, 100mm/s	1.8mA, 250mm/s	2.5mA, 250mm/s
Observation: Over melting observed in all samples					
550˚C	50 reps 10,000mm/s 0.5-6mA, 0.5mm	9mA, 500mm/s	12.5mA, 500mm/s	9mA, 800mm/s	12.5mA, 800mm/s
Observation: Kinetic energy developed by the melt pool pushes excess melt pool off the build region. This material is very loosely sintered powder and is not damaging to the rake. The higher plate heating temperature also seems to be helping in holding the part more firmly to the plate. High scan rates (sample III & IV) prove to be more effective at reduce balling. Low scanning speeds (sample I & II) also seem to permit the beam to melt deeper into the part. Swelling of the surface was also observed in these samples Sample III had the cleanest finish; though overmelting seemed to be occurring in all the samples.					
550˚C	30 reps 10,000mm/s 0.5-6mA, 1mm	9mA, 1000mm/s	12.5mA, 1000mm/s	9mA, 1300mm/s	12.5mA, 1300mm/s
Observation: The objective of this experiment was to minimize the time spent preheating (also increases powder recovery) and improve the surface finish of the part by speeding up the melting and reducing overmelting. It was observed that the sintering during preheating can further be reduced. The parts obtained during this experiment also showed strong evidence of overmelting.					
550˚C	30 reps 10,000mm/s 0.5-5mA, 1.2mm	9mA, 2000mm/s	12.5mA, 2000mm/s	9mA, 3000mm/s	12.5mA, 3000mm/s
Observation: Samples I & II exhibit swelling of the top surface and this is more prominent in sample II. Sample II & IV have a relatively flat top surface but they might have a small amount of porosity as small pinholes were observed in the top surface.					
550˚C	30 reps 10,000mm/s 0.5-5mA, 1.2mm	9mA, 2000mm/s	12.5mA, 2000mm/s	9mA, 3000mm/s	12.5mA, 3000mm/s
Observation: THESE EXPERIMENT WAS CONDUCTED WITH A SLICE THICKNESS OF 0.1MM IN ORDER TO SPEED UP THE PROCESS. It was observed that the surface of the samples was not as flat as those obtained in the previous experiment. The excess melt pool build up was also higher. It was decided that for the current set of experiment it would be more appropriate to use a slice thickness of 0.07mm.					

Table 3 Tensile Test EBM Processing Conditions

Start Plate Temp	Preheat	Sample I-I	Sample I-II	Sample II-I	Sample II-II
550˚C	30 reps 10,000mm/s 0.5-6mA	9mA, 3000mm/s	12.5mA, 3000mm/s	9mA, 2000mm/s	12.5mA, 2000mm/s

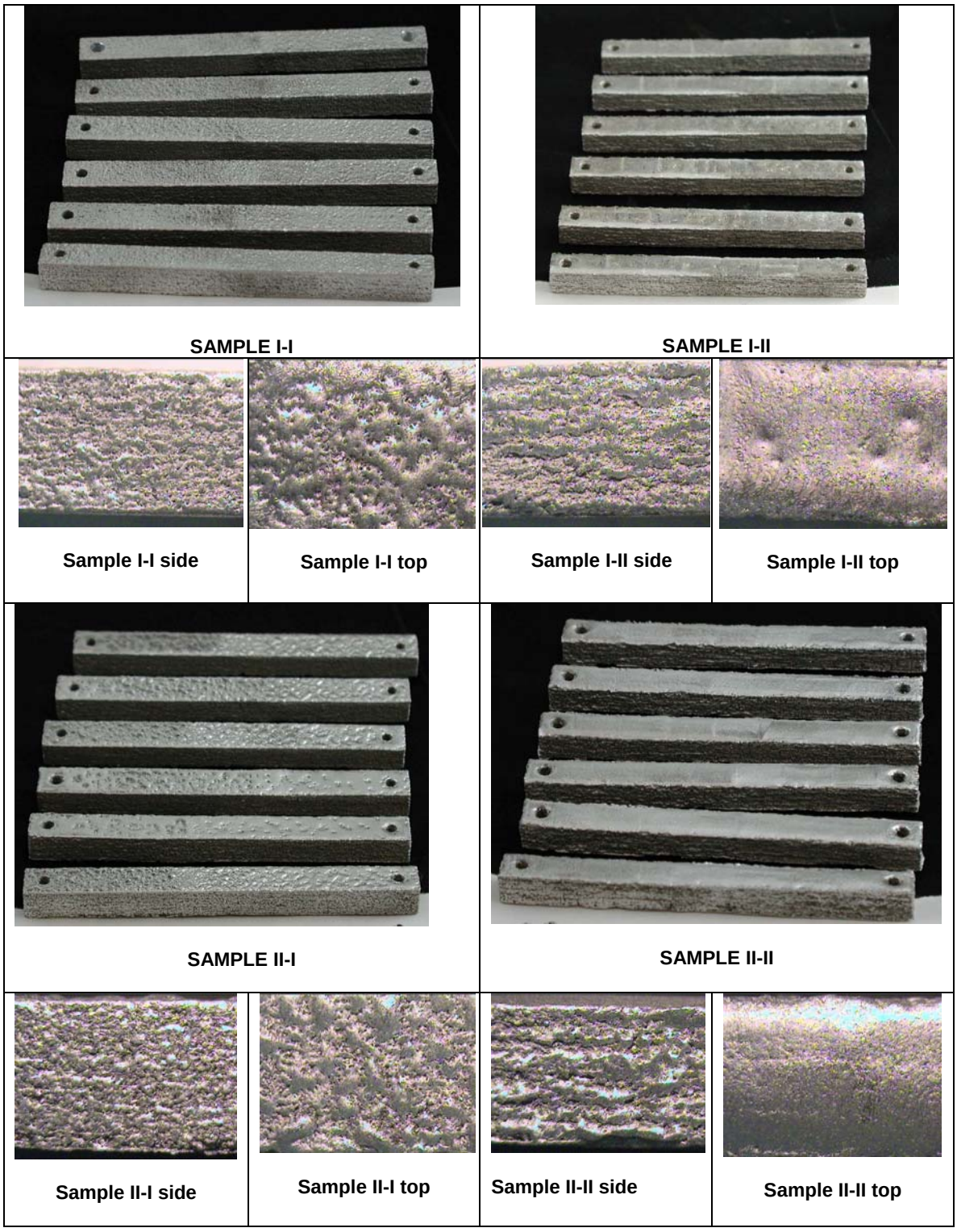

Figure 2 2024 Aluminum Tensile Test Coupons

Table 4 Tensile Coupon Density Approximations

	SAMPLE I-I	SAMPLE I-II	SAMPLE II-I	SAMPLE II-II
DENSITY	2.273g/cc	2.512g/cc	2.425g/cc	2.519g/cc
POROSITY	18.25%	9.635%	12.787%	9.383%

The final step in the initial feasibility study was to produce a complex geometry shape with steep overhanging surfaces. In order to do this, the complex turbocharger wheel shown in Figure 3 was fabricated, as was the set of lattice structures shown in Figure 4. The processing parameters used were same as those for Sample I-I in Table 3.

Figure 3 Aluminum Turbocharger Wheels

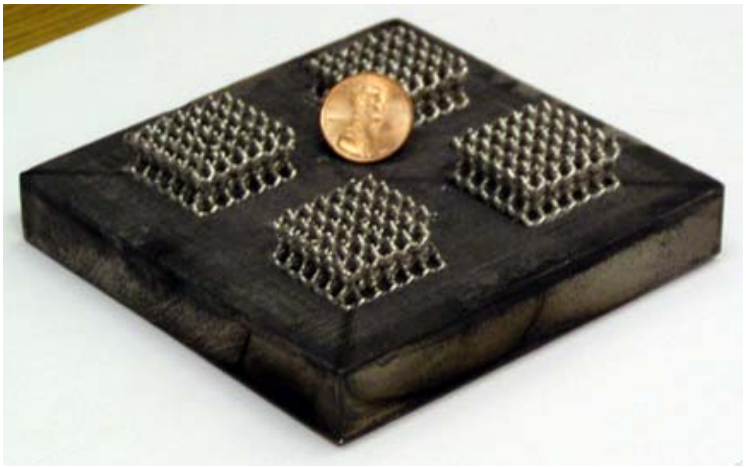

Figure 4 2024 Aluminum Lattice Structures

Electron Beam Melting of 7075 Aluminum

7075 aluminum is a very high strength alloy that is commonly used to produce structural aircraft components. On a percentage basis, the most significant alloying elements of 7075 aluminum are zinc, magnesium, and copper. These alloys are the basis upon which $Mg(Zn,Cu,Al)_2$ precipitation strengthening takes place. It is well understood that melting metals under vacuum will result in some loss of alloying elements due to vaporization. At 10^{-3} mbar vacuum in the e-beam chamber, zinc vaporizes at roughly 300°C and magnesium vaporizes at roughly 375°C. In comparison, both aluminum and copper vaporize at roughly 1200°C. As the melting temperature of 7075 aluminum is approximately 600°C, it is to be expected that some zinc and magnesium will be lost due to their relatively high vapor pressures. This makes 7075 aluminum a much more challenging alloy to work with in a vacuum environment.

In order to test the basic feasibility of processing 7075 aluminum via the EBM process, powder in the +325/-100 mesh size range was obtained from Valimet. The same experimental layout shown in Figure 1 was used to test a very large range of processing conditions in which beam power, beam velocity, stepover distance, and many other parameters were varied.

In order to get a feel for the magnitude of vaporization that is taking place, a representative sample of 7075 aluminum processed on the Arcam machine was sent to NSL Analytical in Cleveland, OH for chemistry analysis. Table 5 shows chemistry analysis for both the unprocessed 7075 Al powder purchased from Valimet as well as the 7075 Al samples processed in the e-beam machine. For reference purposes, the standard limits for 7075 Al are provided in the rightmost column. All elements of the e-beam processed samples fell within allowable limits with the exception (as expected) of zinc and magnesium.

The good news from these results is that neither the zinc nor the magnesium is completely lost to vaporization. This suggests that the rate at which melting and subsequent solidification takes place is rapid enough to preserve reasonable quantities of those alloying elements. Several potential solutions to this issue are currently being evaluated.

Table 5 Vaporization of Alloying Elements In 7075 Aluminum Feasibility Tests

Element	Powder Feedstock Result	Arcam EBM Sample Result	Standard Requirement
Al	Balance	93.9%	87.1 – 91.4%
Cr	0.2%	0.23%	0.18 – 0.28%
Cu	1.59%	1.75%	1.2 – 2%
Fe	0.22%	0.25%	Max 0.5%
Mg	2.22%	1.53%	2.1 – 2.9%
Mn	0.05%	0.053%	Max 0.3%
Ni	NR	0.016%	NA
Si	0.12%	0.19%	Max 0.4%
Sn	NR	<0.001%	NA
Ti	0.03%	0.031%	Max 0.2%
V	NR	0.011%	NA
Zn	5.64%	2.01%	5.1 – 6.1%
Zr	NR	0.022%	NA

In order to qualitatively assess the degree of porosity in the EBM-processed samples, a number of samples were sectioned, mounted, polished, and examined via optical microscope. Both Figure 5 and Figure 6 show side section views of the samples. The bottom surface shown in Figure 5 is the surface that was in contact with the steel plate upon which the samples were "grown". It is readily apparent that metallurgical bonding and mixing between the steel and aluminum took place. Figure 6 shows two different regions of a sample selected to illustrate the degree and nature of pores that are present in the samples. Each figure includes a 200 µm scale bar. For reference, the deposited layer thickness was 100 µm. The height of each image therefore represents approximately 10 layers of deposited thickness. It is readily apparent from the micrographs that there is complete metallurgical bonding between each deposited layer. Figure 6 also clearly shows grains spanning across multiple layers.

Figures 6a and 6b show that the processes samples do not yet have full density. However, the achieved density at this stage of development has improved substantially from where it was at the start of this effort. An important factor to consider is whether the pores are due primarily to incomplete fusion of the powder particles or whether they are due to heat cracking. Of the two causes of porosity, incomplete fusion is by far the easier challenge to overcome. Figure 6b shows both spherical pores as well as pores that are more elongated and jagged in appearance. It is believed that the spherical pores are primarily the result of incomplete fusion. The long irregular pores are of greater concern, as they could be the result of heat cracking. The causes and remedies for both types of pores will be studied in the course of the full development effort.

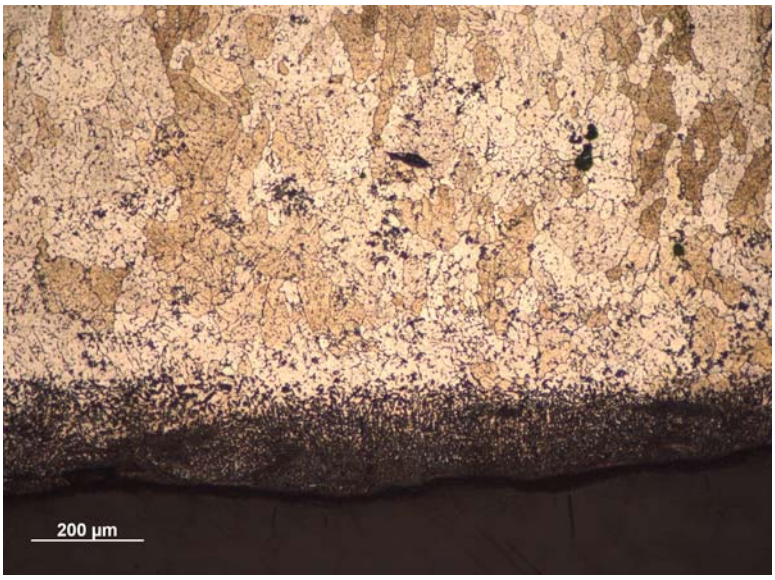

Figure 5 7075 Al Start Plate Interface (10X magnification)

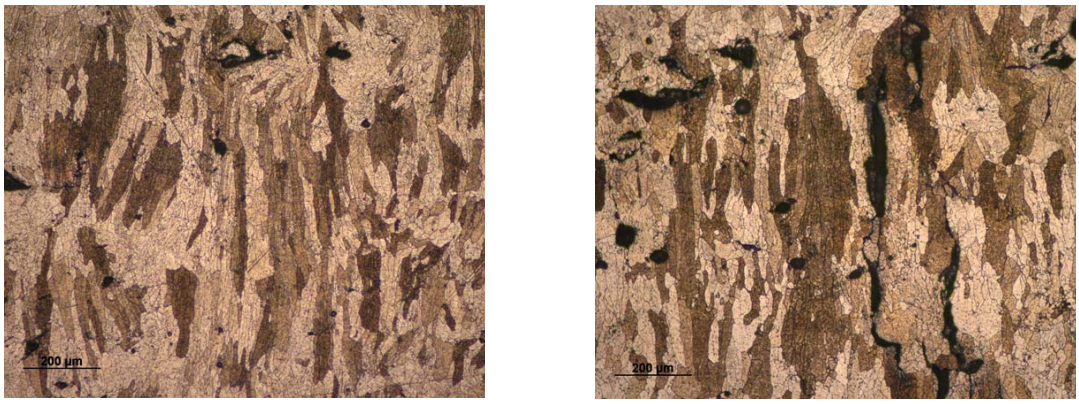

(a) (b)

Figure 6 7075 Grain Structure and Voids (10X magnification)

As of the present time, a small number of geometric shapes have been fabricated in the 7075 aluminum alloy to demonstrate that a basic shape including downward-facing surfaces can be produced. Figures 8 and 9 show simple mechanical shapes, while Figure 10 shows a more complex shape intended for use as a high surface area heat exchanger. Although considerable experimentation remains, initial feasibility results are encouraging.

Figure 7 7075 Aluminum Sample Part

Figure 8 7075 Aluminum Sample Parts

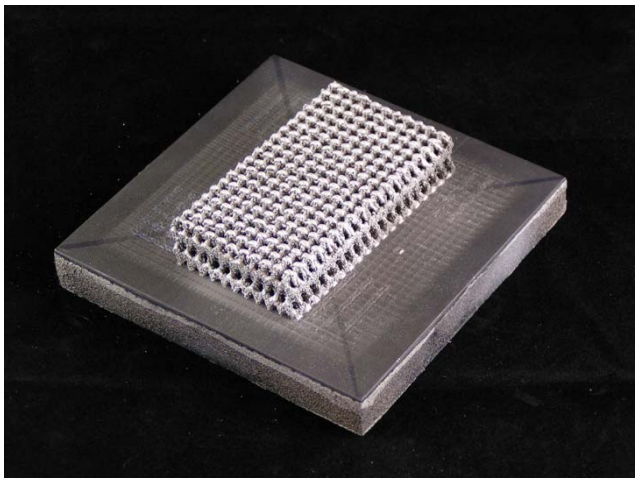

Table 6 7075 Aluminum Lattice Heat Exchanger

Conclusions and Future Work

This paper has described preliminary results of feasibility studies involving direct-metal freeform fabrication of 2024 and 7075 aluminum alloys using the Electron Beam Melting Process. In both cases, initial sets of processing conditions that yielded reasonably good geometric shapes including unsupported downward facing surfaces were located. The primary issues to address in full-scale development efforts include elimination of porosity and control of vaporization of alloying elements.

Acknowledgements

Partial support for these research efforts by NASA and DRS Technical Services is gratefully acknowledged.

References

1. Sercombe, T.B. and G.B. Schaffer, *Rapid manufacturing of aluminum components.* Science, 2003. **301**(5637): p. 1225-1227.

2. Sercombe, T.B. and G.B. Schaffer, *On the role of tin in the infiltration of aluminium by aluminium for rapid prototyping applications.* Scripta Materialia, 2004. **51**(9): p. 905-908.

3. Souveignier, C.W., et al., *Freeform fabrication of aluminum metal-matrix composites.* Journal of materials research, 2001. **16**(9): p. 2613-2618.

4. Matz, J.E., *Carbide formation in a nickel-based superalloy during electron beam solid freeform fabrication*, in *Materials Science and Engineering*. 1999, Massachusetts Institute of Technology: Cambridge MA. p. 94.

5. Taminger, K.M.B. and R.A. Hafley. *Characterization of 2219 aluminum produced by electron beam freeform fabrication*. in *Proceedings of solid freeform fabrication symposium*. 2002. Austin TX: University of Texas, Austin.

6. Watson, J.K., et al. Development of a prototype low voltage electron beam freeform fabrication system. in 13th solid freeform fabrication symposium. 2002. Austin TX: University of Texas, Austin.